

# Evidence That Atypical Protein Kinase C- $\lambda$ and Atypical Protein Kinase C- $\zeta$ Participate in Ras-mediated Reorganization of the F-actin Cytoskeleton

Florian Überall,\* Karina Hellbert,\* Sonja Kampfer,\* Karl Maly,\* Andreas Villunger,\* Martin Spitaler,\* James Mwanjewe,\* Gabriele Baier-Bitterlich,\* Gottfried Baier,<sup>‡</sup> and Hans H. Grunicke\*

\*Institute of Medical Chemistry and Biochemistry and <sup>‡</sup>Institute of Medical Biology and Human Genetics, University of Innsbruck, A-6020 Innsbruck, Austria

**Abstract.** Expression of transforming Ha-Ras L61 in NIH3T3 cells causes profound morphological alterations which include a disassembly of actin stress fibers. The Ras-induced dissolution of actin stress fibers is blocked by the specific PKC inhibitor GF109203X at concentrations which inhibit the activity of the atypical aPKC isotypes  $\lambda$  and  $\zeta$ , whereas lower concentrations of the inhibitor which block conventional and novel PKC isotypes are ineffective. Coexpression of transforming Ha-Ras L61 with kinase-defective, dominant-negative (DN) mutants of aPKC- $\lambda$  and aPKC- $\zeta$ , as well as antisense constructs encoding RNA-directed against isotype-specific 5' sequences of the corresponding mRNA, abrogates the Ha-Ras-induced reorganization of the actin cytoskeleton. Expression of a kinase-defective, DN mutant of cPKC- $\alpha$  was unable to counteract Ras with regard to the dissolution of actin stress fibers. Transfection of cells with constructs encoding constitutively active (CA) mutants of atypical aPKC- $\lambda$  and

aPKC- $\zeta$  lead to a disassembly of stress fibers independent of oncogenic Ha-Ras. Coexpression of (DN) Rac-1 N17 and addition of the phosphatidylinositol 3'-kinase (PI3K) inhibitors wortmannin and LY294002 are in agreement with a tentative model suggesting that, in the signaling pathway from Ha-Ras to the cytoskeleton aPKC- $\lambda$  acts upstream of PI3K and Rac-1, whereas aPKC- $\zeta$  functions downstream of PI3K and Rac-1.

This model is supported by studies demonstrating that cotransfection with plasmids encoding L61Ras and either aPKC- $\lambda$  or aPKC- $\zeta$  results in a stimulation of the kinase activity of both enzymes. Furthermore, the Ras-mediated activation of PKC- $\zeta$  was abrogated by coexpression of DN Rac-1 N17.

**Key words:** Ha-Ras L61 • atypical PKC • F-actin • Rac-1 • PI3K

**E**XPRESSION of transforming Ha-Ras leads to profound morphological alterations which include a disassembly of F-actin stress fibers (Bar-Sagi and Feramisco, 1986; Ridley and Hall, 1992; Prendergast and Gibbs, 1993; Dartsch et al., 1994). Similar effects have been described in Src-transformed cells (Felice et al., 1990; Chang et al., 1995). Ras has been shown to induce changes in cytoskeletal actin through members of the Rho family (Ridley et al., 1992; Rodriguez-Viciana et al., 1994). This family comprises the RhoA, RhoB, and RhoC proteins, Rac-1 and Rac-2, TC10, two CDC42Hs proteins (also known as G25K), RhoG (Hall, 1990; Shinjo et al., 1990;

Ridley and Hall, 1992; Ridley, 1995), and Rnd1 and Rnd-3/RhoE (Nobes et al., 1998). Expression of a dominant-negative (DN)<sup>1</sup> mutant of Rac-1 (Asn-17 Rac1) has been shown to inhibit focus formation and tumorigenesis induced by oncogenic Ras (Qui et al., 1995a,b; Prendergast et al., 1995). Similar findings have been described after expression of a DN Asn-19 RhoB (Prendergast et al., 1995). Expression of Asn-19 RhoB did not interfere with foci formation by Raf-1, indicating that the Ras-RhoB pathway is independent of Raf-1 (Prendergast et al., 1995). The compound SCH 51344 has been described as a suppressor of Ha-Ras-mediated transformation (Kumar et al., 1995) by antagonizing the actin fiber reorganization without in-

F. Überall and K. Hellbert contributed equally to this work.

Address correspondence to F. Überall, Institute of Medical Chemistry and Biochemistry, University of Innsbruck, Fritz Preglstrasse 3, A-6020 Innsbruck, Austria. Tel.: (43) 512-507-3508. Fax: (43) 512-507-2872. E-mail: florian.ueberall@uibk.ac.at

1. *Abbreviations used in this paper:* a, atypical; c, conventional; CA, constitutively active; DN, dominant-negative; GFP, green fluorescence protein; n, novel; PI3K, phosphatidylinositol-3' kinase; PKC, protein kinase C; PVDF, polyvinylidene difluoride.

terference with the growth factor-induced activation of MEK, p44ERK1, or p90<sup>RSK</sup> (Kumar et al., 1995). The data obtained with the DN Rac and Rho mutants and SCH 51344 reverting transformation by Ras emphasize the significance of the Ras-induced reorganization of the actin cytoskeleton for the transformation by the oncogene.

The detailed molecular mechanism by which Ras affects the actin cytoskeleton via Rac and Rho is still insufficiently understood. Microinjection of recombinant, activated RhoA induces actin stress fibers in the absence of added growth factors (Paterson et al., 1990). Serum-induced stress fiber formation can be blocked by the *Clostridium botulinum* exoenzyme C3, an inhibitor of Rho (Rubin et al., 1988; Aktories et al., 1989; Chardin et al., 1989). Actin stress fibers are linked to integrins at the inner surface of the plasma membrane through a multimolecular protein complex called focal adhesion (Burrige et al., 1988). Evidence for an implication of enzymes of the protein kinase C (PKC) family in focal adhesion formation has been reported (Chun and Jacobson, 1992; Vuori and Ruoslahti, 1993; Mogi et al., 1995). Activation of PKC isoenzymes causes a stimulation of cell attachment, spreading, and enhanced tyrosine phosphorylation of focal adhesion kinase, pp125 FAK, a constituent of the focal adhesion complex (Smith-Sinnett et al., 1993). FAK is tyrosine phosphorylated and its tyrosine kinase activity enhanced upon integrin-mediated interaction with the extracellular matrix (Guan et al., 1991; Kornberg et al., 1992; Zachary and Rozengurt, 1992). Enhanced tyrosine phosphorylation of FAK is also observed after exposure to several growth factors (Burrige et al., 1992; Sinnett-Smith et al., 1993; Rankin and Rozengurt, 1994). Thus, FAK may represent a point of convergence where growth factor induced signals meet signals from activated integrins (Zachary and Rozengurt, 1992).

Stimulation of cells by some growth factors like platelet derived growth factor (PDGF), epidermal growth factor (EGF), or insulin has been shown to induce a reorganization of actin filaments by mediating actin polymerization at the plasma membrane, where actin filaments form a compact meshwork resulting in the formation of membrane ruffles and lamellipodia (Mellström et al., 1988; Ridley and Hall, 1992; Rankin and Rozengurt, 1994). Actin filament organization underlying membrane ruffles appears to be mediated by Rac as microinjection of a DN Asn-17 Rac-1 inhibits PDGF-induced membrane ruffles, whereas the constitutively active (CA) Val-12 Rac-1 induces membrane ruffling and the formation of focal complexes (Ridley and Hall, 1992; Qiu et al., 1995a,b). Evidence for an implication of a LIM kinase catalyzed phosphorylation of cofilin in Rac-mediated reorganization of actin cytoskeleton has been presented (Arber et al., 1998; Yang et al., 1998). An additional form of actin filament organization is found in microspikes and filopodia where small bundles of actin filaments are attached to focal complexes at the tips of the filopodia (Nobes and Hall, 1995). Actin filament organization in filopodia appears to be regulated by CDC 42Hs (Nobes and Hall, 1995).

CDC 42-, Rac-1-, and Rho-induced focal complexes are morphologically distinct but share a variety of constituents like vinculin, paxillin, and pp125 FAK (Nobes and Hall, 1995). Evidence for a hierarchical relationship between

CDC 42, Rac and Rho, in which activation of CDC 42 leads to a sequential activation of Rac and Rho has been presented (Nobes and Hall, 1995). The detailed mechanisms, however, regulating the assembly and the spatial organization of the different structures of actin filaments are still insufficiently understood. In view of the similarities between Rho- and Rac-induced focal complexes and the well-documented implication of PKC in the assembly of integrin-containing focal adhesions, a similar role of representatives of the PKC family in the formation of Rac-regulated focal complexes appears conceivable. An implication of enzymes of the PKC family in cytoskeleton organization is supported by a series of published observations (for review see Keenan and Keleher, 1998). The interleukin (IL)-2-mediated alteration of the cytoskeleton has recently been demonstrated to require atypical aPKC- $\zeta$  (Gomez et al., 1997). Transforming Ras has been shown to activate PKC (Morris et al., 1989). Evidence for an implication of atypical aPKC- $\lambda$  in the v-Ras-mediated activation and nuclear translocation of mitogen-activated protein kinase has been presented (Bjorkoy et al., 1997). Induction of c-fos by oncogenic Ras has recently been shown to require the coordinated activities of PKC- $\lambda$ , PKC- $\epsilon$ , and PKC- $\zeta$  (Kampfer et al., 1998). However, whether the Ras-mediated reorganization of the actin cytoskeleton is PKC dependent, which PKC isotypes are involved, and what their function in the Ras-mediated restructuring of the cytoskeleton is, has remained unclear.

In this paper evidence is presented for an implication of the two atypical PKC- $\lambda$ , and PKC- $\zeta$  isotypes in the Ras-mediated reorganization of the actin cytoskeleton. The data support a tentative model for a signaling pathway in which aPKC- $\lambda$  acts downstream of Ras but upstream of phosphatidylinositol-3' kinase (PI3K) and Rac-1, whereas aPKC- $\zeta$  functions downstream of Rac-1.

## Materials and Methods

### Reagents and Plasmids

Dulbecco's modified Eagle's medium (DME) and restriction enzymes for molecular biological approaches were purchased from Boehringer Mannheim. Fetal calf serum and L-glutamine were obtained from BioWhittaker. Leupeptin, myelin basic protein (M-1891), tetramethylrhodamine-isothiocyanate (TRITC)-labeled phalloidin, and aprotinin are products from Sigma. Lipofectin transfection reagents and Opti-Mem I medium were purchased from Life Technologies. [ $\gamma$ -<sup>32</sup>P]ATP (10 mCi/ml, 3000 Ci/mmol) and Hyperfilm-MP were obtained from Amersham. PCR primers used for subcloning strategy were obtained from ARK Scientific.

Subcloning strategy and oligonucleotides used for antisense constructs had been described elsewhere (Kampfer et al., 1998). Orientation of insertion was determined by restriction analysis and sequencing. Subcloning strategy, mutagenic primers, as well as selection primers for the generation of kinase-defective, DN, as well as CA mutants of PKC isotypes had been described elsewhere (Baier-Bitterlich et al., 1996; Überall et al., 1997; Kampfer et al., 1998). All cDNAs for PKC isotypes, green fluorescence protein (GFP), and the cDNA for Rac-1 N17 were subcloned into the expression vector pEF-1neo. GF109203X, LY294002, wortmannin, and Pansorbin beads were obtained from Calbiochem-Novabiochem.

### Cell Culture and Transient Transfection Procedures

NIH3T3 fibroblasts were kept at logarithmic growth phase in DME supplemented with 10% heat-inactivated fetal calf serum, lysophosphatidic acid (100 ng/ml), and 2 mM L-glutamine in a humidified atmosphere containing 5% CO<sub>2</sub>. To obtain transient transfectants, NIH3T3 cells (5 × 10<sup>4</sup> cells per well) were seeded in 100-mm-diam wells containing circular glass

coverslips (eight per well) and were transfected for 8 h with 1  $\mu$ g pEF-1neoGFP expression plasmid, 1.5  $\mu$ g pSR- $\alpha$ II L61 Ha-Ras (encoding a constitutively active Ras leucine L61 mutant), and 20  $\mu$ g of plasmids encoding for kinase-defective, DN cPKC- $\alpha$  K368R, atypical aPKC- $\lambda$  K275W, and aPKC- $\zeta$  K275W mutants. Alternatively, NIH3T3 fibroblasts were cotransfected with plasmids encoding pEF-1neoGFP plus a CA aPKC- $\lambda$  A119E, (CA) aPKC- $\zeta$  A119E, and (CA) cPKC- $\alpha$  A25E mutants, or vector controls (pEF-1neo), respectively.

### Fluorescence Imaging

48 h after the transfection procedure cells were washed twice with PBS (140 mM NaCl, 2.7 mM KCl, 4.6 mM  $\text{Na}_2\text{HPO}_4 \cdot 12 \text{H}_2\text{O}$ , 1.3 mM  $\text{NaH}_2\text{PO}_4 \cdot \text{H}_2\text{O}$ ), fixed with 3.5% formaldehyde (wt/vol in PBS, 10 min) at room temperature and after extensive washing, permeabilized for 5 min with ice-cold acetone. After permeabilizing, the coverslips were washed twice with PBS and incubated for 1 h with FACS<sup>®</sup> buffer (500 ml PBS, 1 g sodium azide, and 4% fetal calf serum). For visualizing the F-actin structure, assembly cells fixed onto glass coverslips were overlaid with 100  $\mu$ l (0.1 g/ml) TRITC-conjugated phalloidin per coverslip for 1 h. Afterwards the stained cells were washed six times with PBS and with distilled water and mounted in Mowiol containing 0.1% (wt/vol) *p*-phenylenediamine.

Mounted cells were viewed on an Olympus BX50 fluorescence microscope, and images of green fluorescence-positive cells were done by using a RGB-mode video real-color camera (Optronics Engineering DEI-470). Image processing was carried out with the image processing software MetaMorph (Princeton Instruments). The green and red fluorescence images were recorded separately by changing the excitation wavelength (from 480 to 550 nm), exported into Adobe Photoshop, and then printed on a color laser copier system (Agfa 707).

### Measurement of Total F-actin Fiber Length

Total F-actin fiber length was calculated after digitalizing TRITC-phalloidin stained F-actin by using the MetaMorph image processing software. The edges of the cells were detected by the aid of a convolution kernel comparing the brightness of the neighboring pixels. After thresholding and separating from the background specimen, fiber lengths were determined and expressed as the percentage of the mean fiber length compared with the fiber length of mock-transfected fibroblasts.

### Partial Purification of 6 $\times$ His-tagged PKC Isootypes and PKC In Vitro Assays

African green monkey kidney fibroblasts (COS-1, 10<sup>6</sup>/100-mm dish) were transfected with 15  $\mu$ g of circular plasmid DNA per dish by lipofectin reagents, as described by the manufacturer. 48 h posttransfection, cells were lysed in 1 ml lysis buffer (150 mM NaCl, 20 mM *N*-2-hydroxyethylpiperazine-*N'*-2-ethanesulfonic acid [HEPES, pH 7.59], 1% Nonidet P-40 (vol/vol), 50  $\mu$ g/ml each aprotinin and leupeptin, and 1 mM phenyl-methylsulfonyl fluoride). Lysates were purified by using a Ni<sup>2+</sup>-resin batch procedure, and equal amounts of recombinant PKC isoatypes were subjected to an enzymatic PKC assay as described elsewhere (Baier-Bitterlich et al., 1996; Überall et al., 1997; Kampf et al., 1998). Enzyme activities of recombinant PKC-isoatypes  $\alpha$ ,  $\lambda$ , and  $\zeta$  are expressed as cofactor-dependent phosphorylation of the [A25S] synthetic PKC peptide (RFARKGSLRQKNVY; presenting the pseudosubstrate sequence of PKC- $\alpha$  with an alanine to serine substitution). The concentrations of substrate peptide and cofactors used are: 50  $\mu$ g/ml [A25S], 280  $\mu$ g/ml PtdSer, 10  $\mu$ M TPA, and 1 mM  $\text{CaCl}_2$ . Expression of the fusion tag peptide COOH-terminal of PKC- $\alpha$  and PKC- $\lambda$  and PKC- $\zeta$  did not affect the kinase activity in vitro (Überall et al., 1997).

### Magnetic Separation of Transiently Transfected COS-1 Cells and PKC- $\zeta$ Immunocomplex Kinase Assay

COS-1 cells cotransfected with pMACS4 (Miltenyi Biotech, 1.5  $\mu$ g), and therefore expressing a truncated CD4 surface marker, were washed twice with PBS and then incubated with PBE (PBS with 5 mM EDTA and 0.5% skimmed milk powder) for 10 min at 37°C to detach cells from the cell culture dish. Suspended cells were incubated for 45 min, 4°C with MACS4 magnetic microbeads (diluted 1:10 in PBE) at 4°C and the positive-transfected cells were separated from the nontransfected background over magnetic columns. Magnetically separated COS-1 cells were washed with cold PBS and lysed on ice in 500  $\mu$ l of lysis buffer A (50 mM Tris-HCl, pH

7.3, 50 mM NaCl, 5 mM  $\text{Na}_4\text{P}_2\text{O}_7 \cdot 10 \text{H}_2\text{O}$  (NaPP), 5 mM EDTA, 2% Nonidet P-40, 25  $\mu$ g/ml leupeptin, 25  $\mu$ g/ml aprotinin, 50 mM NaF, and 100 mM  $\text{Na}_3\text{VO}_4$ ) for 10 min and lysates clarified by centrifugation at 10,000 *g* for 5 min 4°C.

Aliquots of cell equivalents containing equal amounts of protein were subjected to an immunoprecipitation (IP) procedure using a corresponding PKC- $\zeta$  antibody purchased from Santa Cruz Biotechnology. IPs were recovered by using Pansorbin beads. PKC- $\zeta$  molecules bound to 35  $\mu$ l of Pansorbin beads, were resuspended in 20  $\mu$ l kinase buffer, and then mixed with 9  $\mu$ g myelin basic protein (Sigma M-1891). The kinase reactions were initiated by the addition of 2  $\mu$ Ci [ $\gamma$ -<sup>32</sup>P]ATP (10 mCi/ml, 3,000 Ci/mmol) and incubation of the tubes by frequent vortexing at 30°C for 30 min. Phosphorylation of myelin basic protein was terminated by the addition of 5  $\mu$ l of 5 $\times$  SDS sample buffer and boiling the samples for 5 min. Probes were analyzed by SDS-PAGE (10%) and transferred to polyvinylidene difluoride (PVDF) membranes (Millipore). Computer-assisted calculation of PKC- $\zeta$  enzyme activities was done after scanning the corresponding PVDF membranes by using the Scanner Controller Sci System.

## Results

### The Reorganization of Actin Cytoskeleton Induced by Transforming Ras Is Antagonized by the Specific PKC Inhibitor GF109203X

NIH3T3 cells transiently transfected with the transforming Ha-Ras L61 oncogene exhibit dramatic morphological differences compared with their nontransfected counterparts. Normal NIH3T3 fibroblasts are spreading on the extracellular matrix, appear flat, and exhibit bundles of actin stress fibers traversing the cell (Fig. 1 A). Cells expressing the Ras oncogene are more spindle-shaped, exhibit frequently long protrusions, and are characteristically devoid of actin stress fibers (Fig. 1 B). Similar morphological effects of transforming Ras have been described by other authors (Bar-Sagi and Feramisco, 1986; Ridley and Hall, 1992; Prendergast and Gibbs, 1993; Dartsch et al., 1994; Rodriguez-Viciana et al., 1994).

As shown in Fig. 1 D, the PKC-specific inhibitor GF109203X (Toullec et al., 1991) is capable of reversing the dissolution of actin stress fibers by Ras. This effect is observed in the presence of 6  $\mu$ M of the inhibitor (Fig. 1 D). 200 nM of the compound which had been shown to be sufficient for blocking c- and n-type PKC isotype kinase activity in cell-free extracts (Fig. 2 A) (Überall et al., 1997), is, however, without an effect on the Ras-mediated stress fiber dissolution (Fig. 1 C). 6  $\mu$ M GF109203X corresponds roughly to the IC<sub>50</sub> of the compound against the atypical PKC- $\zeta$  (Fig. 2 B, see also Martiny-Baron et al., 1993), and as shown in Fig. 2 C, exerts a similar effect on PKC- $\lambda$ , suggesting that if a PKC is involved in the Ras-induced reorganization of the actin cytoskeleton, it should be an atypical (a-), rather than a conventional (c-) or novel (n-) type PKC isoform.

### Reversion of Ras-induced Alteration of Actin Cytoskeleton by Kinase-defective, DN Mutants of Atypical PKC- $\lambda$ , and PKC- $\zeta$ as well as by PKC- $\lambda$ - and PKC- $\zeta$ -specific Antisense Constructs

As shown in Fig. 3, B and D, expression of aPKC- $\lambda$  K275W as well as PKC- $\zeta$  K275W mutants, which contain an inactive ATP-binding site, is able to revert the Ras-induced depolymerization of actin stress fibers. For these experiments NIH3T3 cells were transiently cotransfected with vectors encoding Ha-Ras L61 and kinase-defective,

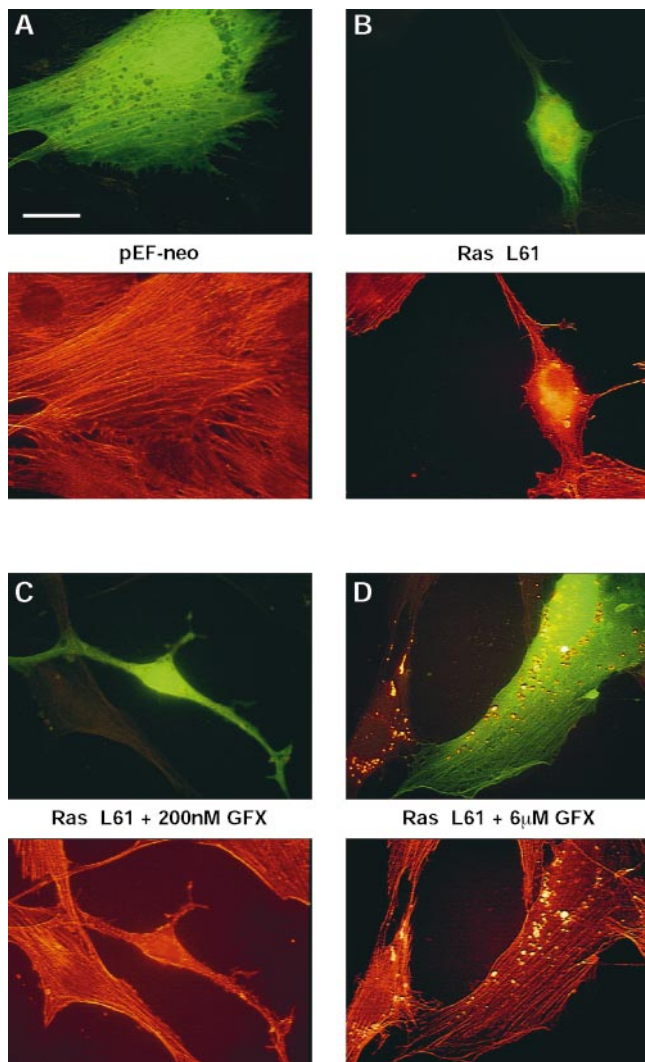


**Figure 1.** Ras L61-induced F-actin stress fiber disassembly is antagonized by the specific PKC inhibitor GF109203X at concentrations sensitive for atypical PKC-isotypes. Representative fluorescence images of green fluorescence protein expression (top panels) versus TRITC-phalloidin-stained fibroblasts (bottom panels), transiently expressing Ha-Ras L61 (B–D). (A) Vector control; (B) Ras L61; (C) Ras L61 in the presence of 200 nM GF109203X; (D) Ras L61 in the presence of 6  $\mu$ M GF109203X. 48 h posttransfection, cells were fixed and expression of GFP was visualized by fluorescence microscopy. F-actin filaments were stained by using TRITC-conjugated phalloidin. Representative cells of at least three different experiments are shown for all panels. Stacks of images were exported into Adobe Photoshop and printed as described in Materials and Methods. Bar, 10  $\mu$ m.

DN aPKC- $\lambda$  K275W or aPKC- $\zeta$  K275W mutants, respectively, using a green fluorescence protein expression vector as a transfection marker. Ras-induced reorganization of F-actin cytoskeleton was not affected by an expression of a kinase-defective, DN mutant of PKC- $\alpha$  K368R (Fig. 3 F). Expression levels of cPKC- $\alpha$  K368R, aPKC- $\lambda$  K275R, and aPKC- $\zeta$  K275R were found to be in a similar range (data not shown).

The effects observed after expression of the DN versions of PKC- $\lambda$  and PKC- $\zeta$  were checked by PKC- $\lambda$ - and

PKC- $\zeta$ -specific antisense constructs. For this purpose, cells were transfected with constructs encoding isotype-specific 5' sequences targeted to the corresponding mRNA. As described previously, generation of these antisense RNA sequences leads to an almost complete depletion of the endogenous aPKC- $\lambda$  and - $\zeta$  (Kampfer et al., 1998).

Fig. 3, C and E demonstrate that isotype-specific depletion of aPKC- $\lambda$  and aPKC- $\zeta$  yields the same results as expression of DN mutants of these isoforms. In agreement with the results obtained with the DN PKC- $\alpha$  mutant, PKC- $\alpha$  antisense did not affect the Ras-mediated alterations of F-actin organization (Fig. 3 G). Neither cPKC- $\alpha$  nor aPKC- $\lambda$ - $\zeta$  sense constructs did affect the Ras-mediated disassembly of F-actin fibers (data not shown).

A quantitative evaluation of Ras-mediated stress fiber depolymerization and the effects of (DN) aPKC- $\lambda$  K275W, (DN) aPKC- $\zeta$  K275W, aPKC- $\lambda$ , and aPKC- $\zeta$  antisense on Ras-induced actin fiber organization was performed by measuring F-actin fiber length with the aid of the MetaMorph image processing software (Fig. 4, A and B).

The data shown in Figs. 3 and 4 clearly indicate that the Ras-mediated alteration of actin cytoskeleton is antagonized by an isotype-specific inhibition or depletion of aPKC- $\lambda$  and aPKC- $\zeta$ . These findings strongly suggest that the Ras-mediated reorganization of the actin cytoskeleton is mediated by these two atypical aPKC isoforms.

#### *Expression of CA Mutants of Atypical aPKC- $\lambda$ and aPKC- $\zeta$ Mimic the Effect of Transforming Ras L61 on Actin Cytoskeleton*

It has previously been demonstrated that substitution of an alanine by a glutamate within the pseudosubstrate domain of PKC isoforms generates CA mutants with reduced cofactor requirements. Biochemical and biological properties of these mutants had been described in preceding publications (Baier-Bitterlich et al., 1996; Überall et al., 1997; Kampfer et al., 1998).

If Ha-Ras uses atypical PKC isoforms for the reorganization of the actin cytoskeleton as suggested by the data shown in Figs. 3 and 4, expression of CA aPKC- $\lambda$  and (CA) aPKC- $\zeta$  mutants should affect actin stress fibers like transforming Ha-Ras. As shown in Fig. 5, B and D, this is indeed the case. A CA mutant of PKC- $\alpha$  A25E did not show any significant effect on stress fiber rearrangements (data not shown).

Stress fibers reappear after treatment of the aPKC- $\lambda$  A119E- or aPKC- $\zeta$  A119E-expressing cells with the PKC inhibitor GF109203X demonstrating that the alterations of the actin cytoskeleton in cells expressing the constitutively active versions of these atypical PKC isoforms are indeed caused by a PKC activity (Fig. 5, C and E).

#### *Evidence That Atypical aPKC- $\lambda$ Acts Upstream and aPKC- $\zeta$ Acts Downstream of Rac-1*

An early event after expression of oncogenic Ras is the generation of membrane ruffles and a reorganization of the actin cytoskeleton, i.e., stress fibers disappear whereas F-actin accumulates at the cell periphery (Bar-Sagi and Feramisco, 1986; Ridley et al., 1992; Rodriguez-Viciana et al., 1994). Evidence for an implication of Rac-1 in Ras-mediated reorganization of the actin cytoskeleton has been pre-

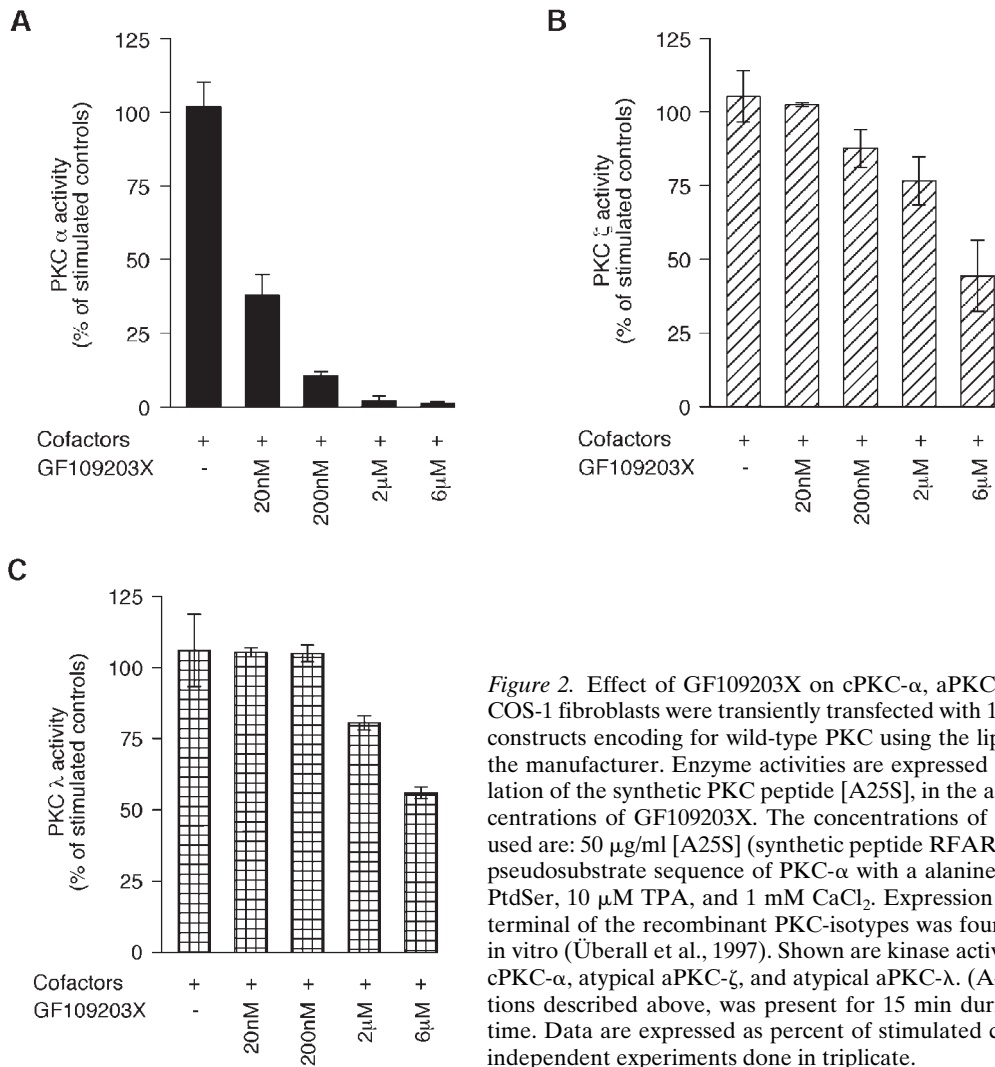


**Figure 2.** Effect of GF109203X on cPKC- $\alpha$ , aPKC- $\zeta$ , and aPKC- $\lambda$  enzyme activities. COS-1 fibroblasts were transiently transfected with 15  $\mu$ g of PKC- $\alpha$ , PKC- $\lambda$ , and PKC- $\zeta$  constructs encoding for wild-type PKC using the lipofectin technique as described by the manufacturer. Enzyme activities are expressed as cofactor-dependent phosphorylation of the synthetic PKC peptide [A25S], in the absence or presence of various concentrations of GF109203X. The concentrations of synthetic substrates and cofactors used are: 50  $\mu$ g/ml [A25S] (synthetic peptide RFARKGSLRQKNVY representing the pseudosubstrate sequence of PKC- $\alpha$  with an alanine-to-serine substitution), 280  $\mu$ g/ml PtdSer, 10  $\mu$ M TPA, and 1 mM CaCl<sub>2</sub>. Expression of the fusion tag-peptide COOH-terminal of the recombinant PKC-isotypes was found not to affect the kinase activity in vitro (Überall et al., 1997). Shown are kinase activities of Ni<sup>2+</sup>-batched recombinant cPKC- $\alpha$ , atypical aPKC- $\zeta$ , and atypical aPKC- $\lambda$ . (A–C) GF109203X, at the concentrations described above, was present for 15 min during the whole PKC assay running time. Data are expressed as percent of stimulated controls ( $\pm$  SEM) of at least three independent experiments done in triplicate.

sented (Ridley et al., 1992; Rodriguez-Viciano et al., 1994). The data described so far suggest that the atypical PKC isotypes  $\lambda$  and  $\zeta$  are also involved in this process. It appeared interesting, therefore, to investigate whether they act within the Ras/Rac pathway and if they do, whether their position within this pathway can be identified.

As should be expected, DN N17 Rac-1 inhibits the Ras-mediated disassembly of stress fibers (Fig. 6, A and B). To obtain some information whether PKC- $\lambda$  and PKC- $\zeta$  cooperate with Rac-1 in the same pathway, cells were cotransfected with combinations of either CA aPKC- $\lambda$  A119E and N17 Rac-1 or CA aPKC- $\zeta$  A119E and N17 Rac-1.

As shown in Fig. 6 C, N17 Rac-1 is able to overcome stress fiber disassembly induced by CA aPKC- $\lambda$  A119E (compare with Fig. 5 for the effect of aPKC- $\lambda$  A119E in the absence of N17 Rac-1), indicating that aPKC- $\lambda$  acts upstream of Rac-1. Stress fiber disassembly by aPKC- $\zeta$  A119E, however, is not affected by N17 Rac-1 (Fig. 6 D), suggesting that aPKC- $\zeta$  acts either downstream or independent of Rac-1. A quantitative evaluation of the stress

fiber alterations shown in Fig. 6 is presented in Fig. 4 B and Fig. 10.

#### *Effects of Transforming Ras and CA Rac on aPKC- $\lambda$ and aPKC- $\zeta$*

The data presented so far suggest that Ras mediates the effects on the cytoskeleton via a pathway containing aPKC- $\lambda$ -Rac-1 and aPKC- $\zeta$ . If this model is correct, Ras should activate aPKC- $\lambda$  and aPKC- $\zeta$  whereas Rac should be able to stimulate aPKC- $\zeta$ . Unfortunately, this question could not be addressed in NIH3T3 cells due to the low transfection efficiencies in this cell type. Therefore, these studies were performed with COS cells. As shown in Fig. 7 A, cotransfection of COS cells with plasmids encoding Ras L61 and 6 $\times$  His-tagged aPKC- $\lambda$  leads to a significant activation of the kinase activity of aPKC- $\lambda$ . Coexpression of Ras L61 and aPKC- $\zeta$  results in a marked stimulation of aPKC- $\zeta$  as demonstrated in Fig. 7 B. Furthermore, cotransfection of a plasmid encoding CA V12Rac with a construct encoding aPKC- $\zeta$  also revealed an activation of

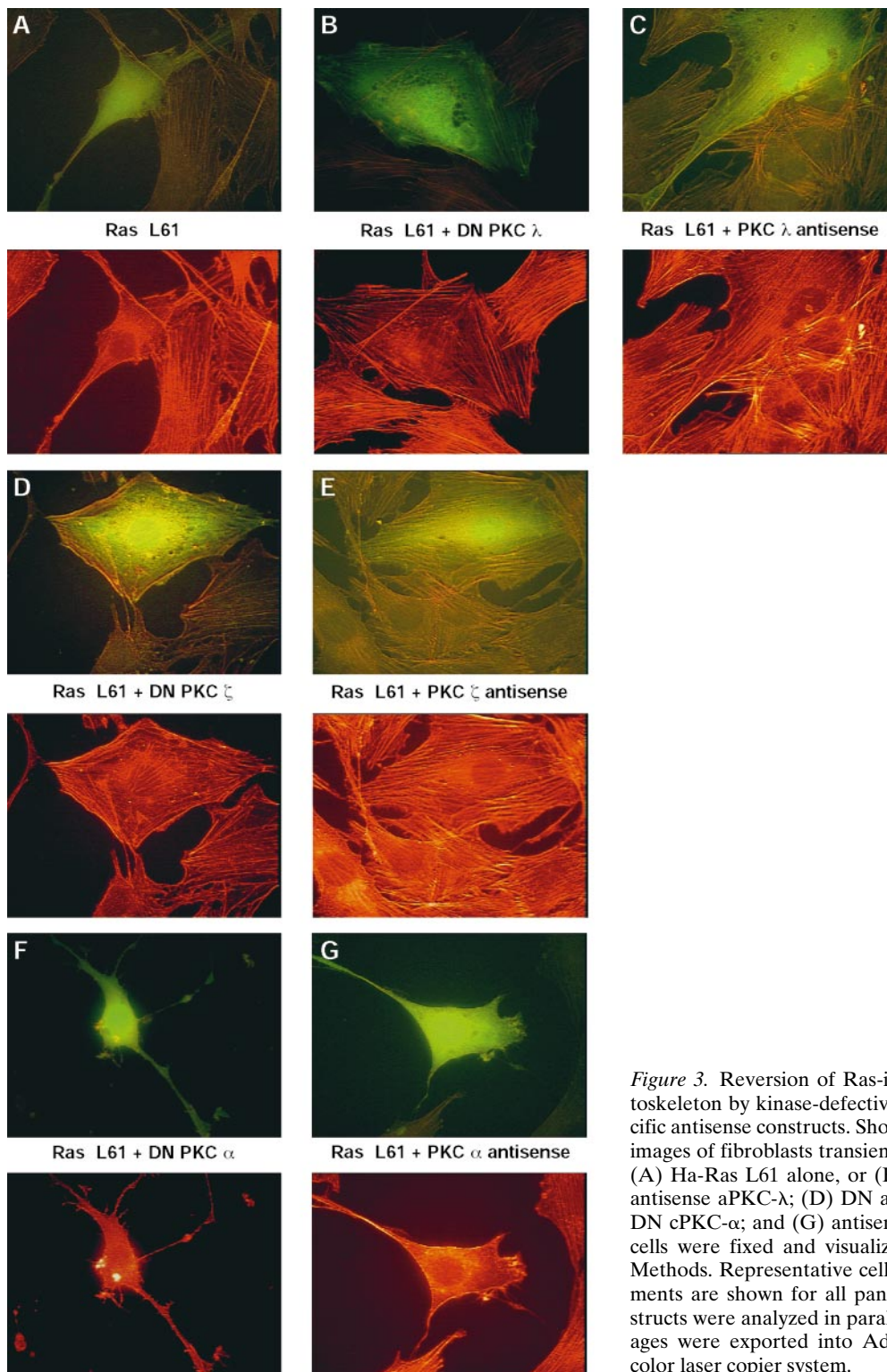


**Figure 3.** Reversion of Ras-induced disassembly of F-actin cytoskeleton by kinase-defective, DN as well as PKC isotype-specific antisense constructs. Shown are representative fluorescence images of fibroblasts transiently expressing Ha-Ras L61 (A–G). (A) Ha-Ras L61 alone, or (B) together with DN aPKC- $\lambda$ ; (C) antisense aPKC- $\lambda$ ; (D) DN aPKC- $\zeta$ ; (E) antisense aPKC- $\zeta$ ; (F) DN cPKC- $\alpha$ ; and (G) antisense cPKC- $\alpha$ . 48 h posttransfection, cells were fixed and visualized as described in Materials and Methods. Representative cells of at least three different experiments are shown for all panels. The corresponding sense constructs were analyzed in parallel (data not shown). Stacks of images were exported into Adobe Photoshop and printed on a color laser copier system.

aPKC- $\zeta$  by Rac (Fig. 7 C). Surprisingly, V12Rac in addition to aPKC- $\zeta$  also activated aPKC- $\lambda$  (data not shown). However, this finding is not in conflict with data or models presented so far. Possible interpretations for this effect will be presented in the Discussion. Our conclusion that

Ras activates aPKC- $\zeta$  by a Rac-1-dependent mechanism is supported by the fact that expression of DN N17Rac blocks Ras-mediated stimulation of aPKC- $\zeta$  (Fig. 7 D). N17Rac does not inhibit Ras-mediated activation of PKC- $\lambda$  (data not shown).

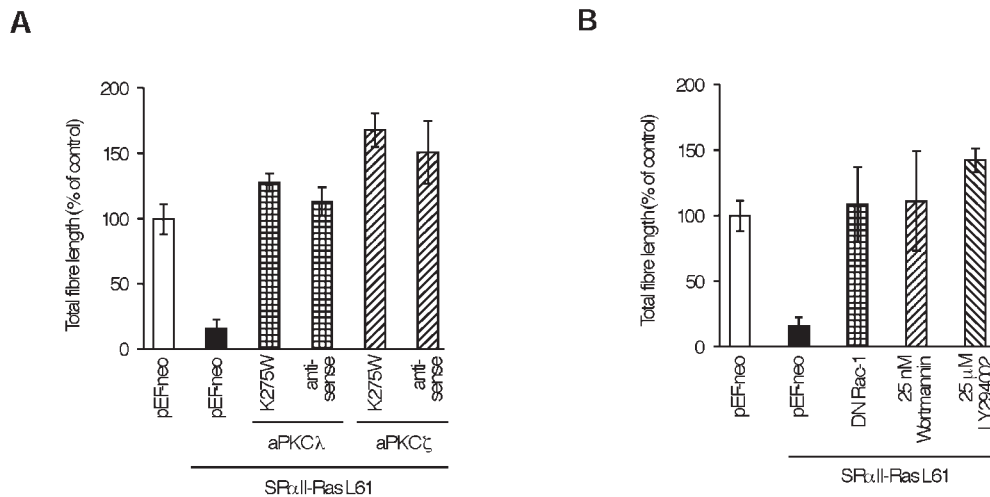


**Figure 4.** Quantitative evaluation of total fiber length. Effects of kinase-defective, DN PKC-isotypes. Total F-actin fiber length was calculated after digitalizing TRITC-phalloidin stained F-actin by using the MetaMorph image processing software S/N 3542A. The edges of the cells were detected by the aid of a convolution kernel. This means that the brightness of the neighboring pixels were compared. After thresholding and separating from the background specimen, fiber lengths were calculated and expressed as the means of total fiber length compared

with the fiber length of mock-transfected fibroblasts. Shown are morphological alterations of Ras-mediated stress fiber disassembly under the influence of (A) (DN) aPKC- $\lambda$  K275W, antisense aPKC- $\lambda$ , (DN) aPKC- $\zeta$ , antisense aPKC- $\zeta$ , and (B), (DN) N17 Rac-1, and the PI3K inhibitors wortmannin and LY294002. Bars indicate means ( $\pm$  SEM) of at least three independent experiments with  $\sim$ 60–75 GFP-positive cells which were separately analyzed per coverslip.

### Effect of PI3K Inhibitors on Actin Cytoskeleton Reorganization Induced by Oncogenic Ras or CA Mutants of aPKC- $\lambda$ and aPKC- $\zeta$

PI3K has been shown to be implicated in the Ras-induced reorganization of actin cytoskeleton (Rodriguez-Viciano et al., 1994). In agreement with these findings, treatment of Ras-expressing cells with the PI3K inhibitors wortmannin or LY294002 counteracts the effects of Ras on the actin cytoskeleton (Fig. 8). Both inhibitors also antagonize the disassembly of actin stress fibers induced by constitutively active aPKC- $\lambda$  A119E, whereas the cytoskeletal reorganization mediated by the aPKC- $\zeta$  A119E mutant was not affected (Fig. 9). These data suggest that aPKC- $\lambda$  acts upstream of PI3K whereas aPKC- $\zeta$  functions either downstream or independent of PI3K. A quantitative evaluation of the effects of the PI3K inhibitors is presented in Fig. 4 B and Fig. 10.

### Discussion

The data presented here demonstrate that transforming Ha-Ras uses atypical aPKC- $\lambda$  and aPKC- $\zeta$  for the rearrangement of actin cytoskeleton. This conclusion is based on the observation that (a) the Ha-Ras-induced dissolution of actin stress fibers is blocked by the specific PKC inhibitor GF109203X at concentrations which inhibit the activity of the atypical aPKC isotypes  $\lambda$  and  $\zeta$ . (b) Coexpression of transforming Ha-Ras L61 with kinase-defective, DN mutants of aPKC- $\lambda$  and aPKC- $\zeta$ , as well as antisense constructs encoding RNA directed against isotype-specific 5' sequences of the corresponding mRNAs, abrogate the Ha-Ras-induced reorganization of the actin cytoskeleton. (c) Finally, transfection of cells with constructs encoding CA mutants of atypical aPKC- $\lambda$  and aPKC- $\zeta$  mimic the effect of oncogenic Ha-Ras on actin cytoskeleton reorganization.

With regard to the effects of the PKC inhibitor GF109203X, it may appear surprising that concentrations of the inhibitor which, *in vitro*, reduce the activity of aPKC- $\lambda$  and aPKC- $\zeta$  to  $\sim$ 50% cause an almost complete reversal of the Ras-mediated disassembly of F-actin stress fibers. It should be emphasized, however, that neither the biological activators nor the intracellular substrates of atypical PKC isozymes have been sufficiently identified. Thus, the reaction mixtures used for the determination of the enzyme activity of the two kinases certainly differ from the *in vivo* conditions and this may affect the sensitivity to the inhibitor. Furthermore, both aPKC- $\lambda$  and aPKC- $\zeta$  are affected by the inhibitor to about the same extent, i.e.,  $\sim$ 50%. Since both enzymes are required for the Ras-mediated restructuring of actin cytoskeleton, the simultaneous inhibition of both enzymes may result in an additive effect. Finally, the intracellular concentration of the inhibitor is not known. It is possible, therefore, that locally higher concentrations than 6  $\mu$ M have been achieved.

Expression of a kinase-defective, DN mutant of PKC- $\alpha$  or PKC- $\alpha$  depletion by intracellular generation of PKC- $\alpha$  antisense RNA did not affect the Ras-induced alterations of the actin cytoskeleton. In a previous paper we had demonstrated that the phosphorylation of MARCKS in NIH3T3 cells under biological conditions is mediated by PKC- $\alpha$  and that the phorbol ester-induced phosphorylation of MARCKS is markedly inhibited by expression of the kinase-defective, DN PKC- $\alpha$  K368R mutant (Überall et al., 1997). Thus, the inability of PKC- $\alpha$  K368R to interfere with the Ras-induced effects on actin cytoskeleton is not explained by an insufficient intracellular expression level. Furthermore, the phosphorylation of MARCKS, which has been discussed as an important regulator of actin organization (Rosen et al., 1990), does not appear to be involved in the Ras-induced reorganization of the actin cytoskeleton.

The Ras-induced reorganization of actin cytoskeleton

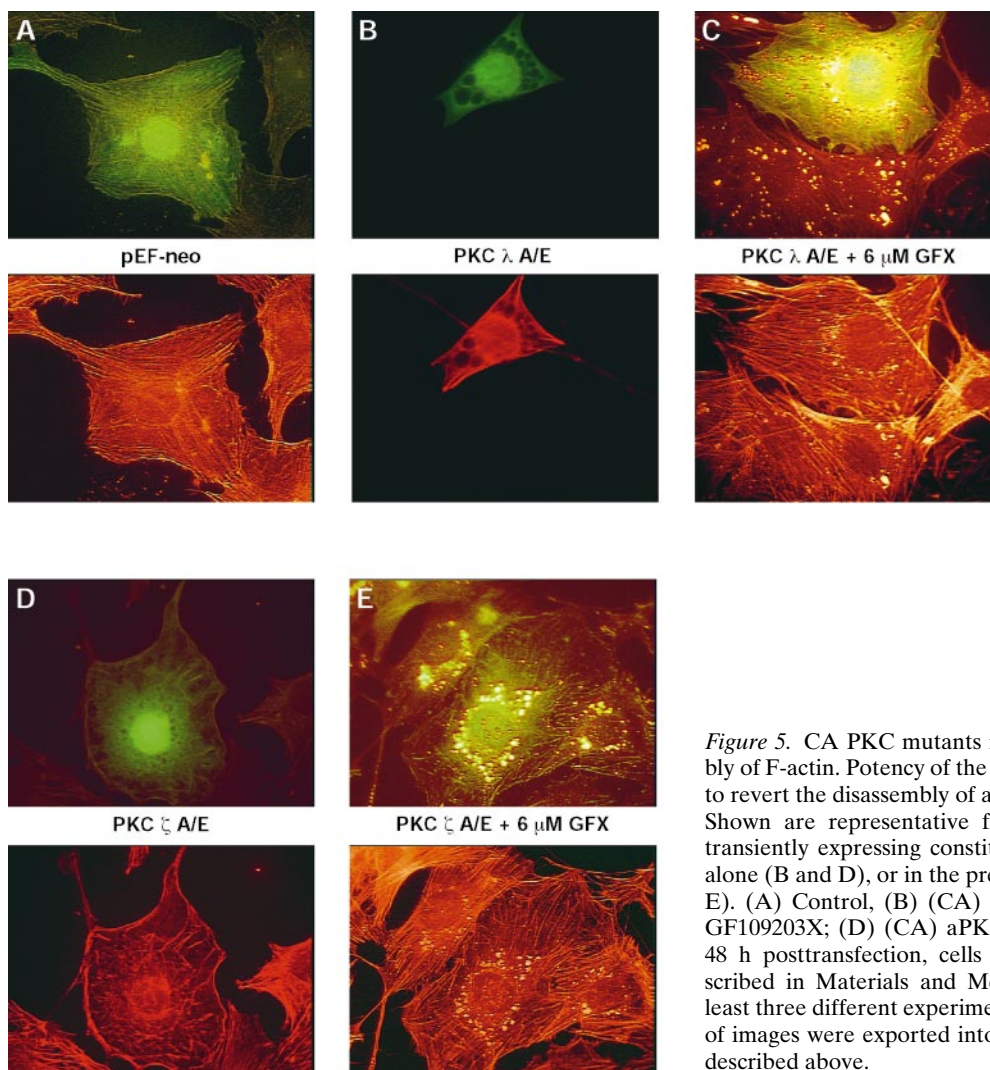


**Figure 5.** CA PKC mutants mimic the Ras-mediated disassembly of F-actin. Potency of the PKC-specific inhibitor GF109203X to revert the disassembly of actin fibers induced by CA mutants. Shown are representative fluorescence images of fibroblasts transiently expressing constitutively active (CA) PKC mutants alone (B and D), or in the presence of 6  $\mu$ M GF109203X (C and E). (A) Control, (B) (CA) atypical aPKC- $\lambda$  A119E; (C) plus GF109203X; (D) (CA) aPKC- $\zeta$  A119E; (E) plus GF109203X. 48 h posttransfection, cells were fixed and visualized as described in Materials and Methods. Representative cells of at least three different experiments are shown for all panels. Stacks of images were exported into Adobe Photoshop and printed as described above.

has been shown to be mediated by Rac-1 and PI3K (Jones and Bar-Sagi, 1997). The data presented here suggest that aPKC- $\lambda$  acts upstream of PI3K and Rac-1, whereas aPKC- $\zeta$  functions either downstream or independent of Rac-1. This conclusion is based on the following findings: (a) the effects of the constitutively active mutant of aPKC- $\lambda$  which mimics Ras with regard to the alterations of actin cytoskeleton are inhibited by the PI3K blockers wortmannin and LY294002 and also by expression of DN N17 Rac-1; and (b) expression of N17 Rac-1 does not interfere with the disassembly of actin stress fibers induced by the CA aPKC- $\zeta$  A119E mutant. The sequence Ras-aPKC- $\lambda$ -PI3K-Rac-1 would be in accordance with the model suggested by Rodriguez-Viciana et al. (1994), who propose a pathway in which the Ras-mediated activation of Rac-1 is mediated by PI3K. Our findings would add atypical aPKC- $\lambda$  as an upstream element of this sequence, a model consistent with data demonstrating a physical interaction of aPKC- $\lambda$  with p21ras (Diaz-Meco et al., 1994).

The studies presented here demonstrate that in intact cells, Ras is capable of activating aPKC- $\lambda$ . Furthermore, it is shown here that in addition to the stimulation of

aPKC- $\lambda$ , Ras also enhances the kinase activity of aPKC- $\zeta$ . The latter effect is suppressed in cells expressing DN N17Rac. We conclude, therefore, that Ras activates aPKC- $\zeta$  by a Rac-1-dependent mechanism. This conclusion is supported by the finding that expression of constitutively active V12Rac enhances the kinase activity of aPKC- $\zeta$ . Surprisingly, V12Rac was also found to be capable of activating aPKC- $\lambda$ . However, this observation is not in conflict with the other data presented in this paper, and does also not contradict a model suggesting that the effects of Ras on actin cytoskeleton are mediated by a pathway comprising aPKC- $\lambda$ -Rac-aPKC- $\zeta$ . The fact that in COS cells V12Rac can activate aPKC- $\lambda$  indicates that an activation of Rac-1 by a Ras-independent pathway, e.g., via CDC 42, may lead to a Rac-mediated activation of aPKC- $\lambda$  and aPKC- $\zeta$ . This is obviously in contrast to the pathway activated by oncogenic Ras where aPKC- $\lambda$  acts upstream and aPKC- $\zeta$  downstream of Rac as outlined above. A conclusion which is also supported by the observation that in COS cells DN N17Rac does not interfere with Ras-mediated activation of aPKC- $\lambda$ .

As the mechanism by which Ras affects actin filament



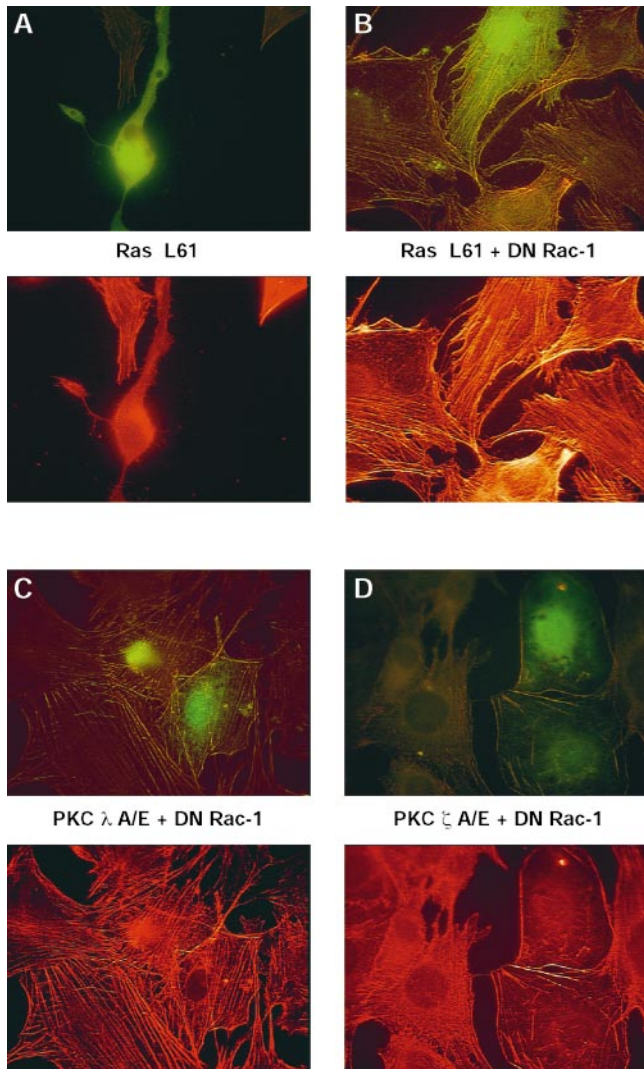


**Figure 6.** Evidence that atypical aPKC- $\lambda$  acts upstream and aPKC- $\zeta$  acts downstream of Rac-1. Shown are representative fluorescence images of fibroblasts transiently expressing Ha-Ras L61 (A and B). (A) Ha-Ras L61 alone, or (B) together with DN Rac-1 N17; (C) (CA) aPKC- $\lambda$  A119E together with (DN) Rac-1 N17; or (D) (CA) aPKC- $\zeta$  A119E together with (DN) Rac-1 N17. 48 h posttransfection, cells were fixed and visualized as described in Materials and Methods. Representative cells of at least three different experiments are shown for all panels. Stacks of images were exported into Adobe Photoshop and printed on a color laser copier system.

structures are incompletely understood, it can be only speculated with regard to the function of aPKC- $\lambda$  or aPKC- $\zeta$  in this pathway. The disassembly of actin stress fibers has been correlated to the accumulation of inactive, GDP-charged RhoA (Qui et al., 1995a,b). Activation of RhoA by an exchange of the GDP by a GTP was found to stimulate stress fiber formation (Ridley and Hall, 1992). These findings suggest that the Ras-induced disassembly of actin stress fibers is the result of a conversion of the active, GTP-charged Rho to the inactive GDP-bound form. Models for a biochemical linkage between the Ras and Rho proteins have been proposed (Boguski et al., 1992;

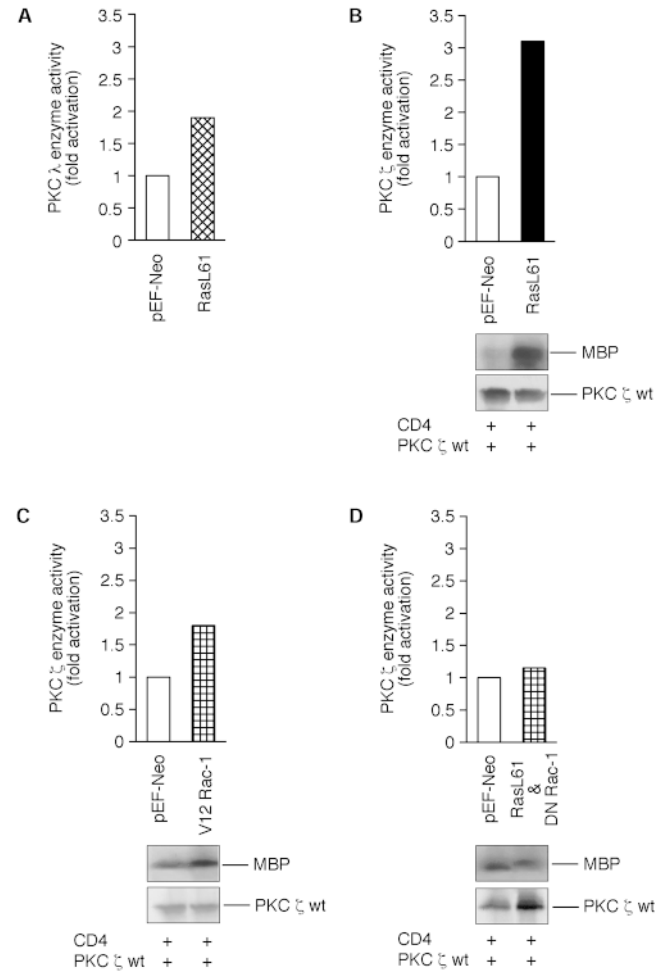


**Figure 7.** Effects of oncogenic Ras and constitutively active Rac on kinase activities of aPKC- $\zeta$  and aPKC- $\lambda$ . Shown are representative immunocomplex kinase assays (B–D) and an in vitro kinase assay (A) of magnetically separated COS-1 cells. The data are designed as bar graphs (top panels) and as corresponding autoradiograms of the myelin basic protein (MBP) assay (bottom panels). Equal amounts of recombinant proteins used in the experiment were employed using a standard Western blotting technique as described by Kampfer et al. (1998). In brief, logarithmically growing cells were transiently cotransfected with (A) Ha-Ras L61 together with aPKC- $\lambda/\zeta$ , (B) Ha-Ras L61 together with aPKC- $\zeta$ , (C) CA Rac-1 V12 together with aPKC- $\zeta$ , and (D) DN Rac-1 N17 together with aPKC- $\zeta$ . Concerning magnetic bead separation of positively transfected cells, a truncated CD4 surface marker was cotransfected in B and C. 48 h posttransfection, cells were separated by using magnetic beads as described by the manufacturer and PKC assays were done as described under Materials and Methods. Enzyme activities are expressed as cofactor-independent phosphorylation of (A) a synthetic PKC- $\alpha$  peptide (A25S, for details see Fig. 2 legend) or myelin basic protein (B–D). Computer-assisted calculation of PKC- $\zeta$  or PKC- $\lambda$  activities were done after scanning the corresponding PVDF membranes by using the Scanner Controller Sci System.

Nobes and Hall, 1994; Chant and Stowers, 1995). In one simple model, the Ras/Rho pathway includes p120<sup>GAP</sup>, the Ras GTPase-activating protein which may also act as a Ras effector (Chant and Stowers, 1995) and p190, a p120<sup>GAP</sup>-associated protein which exhibits a Rho-specific

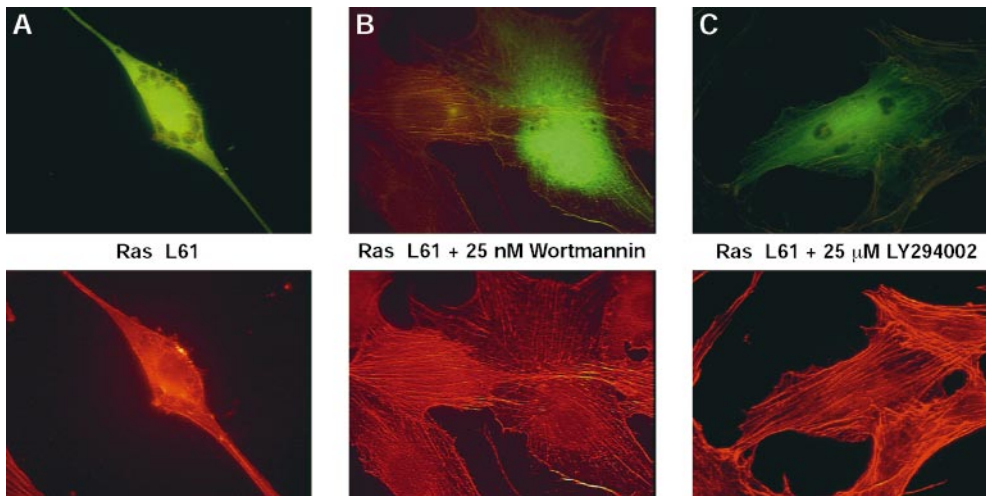


**Figure 8.** Treatment of Ras-expressing cells with the PI3K inhibitors wortmannin or LY294002 counteracts the effects of Ras on the actin cytoskeleton. Shown are representative fluorescence images of fibroblasts transiently expressing Ha-Ras L61. (A) Ha-Ras L61 alone, or (B) in the presence of 25 nM wortmannin, or (C) in the presence of 25  $\mu$ M LY294002. 48 h posttransfection, cells were fixed and visualized as described in Materials and Methods. Representative cells of at least three different experiments are shown for all panels. Stacks of images were exported into Adobe Photoshop and printed as described.

GTPase-activating domain (Settleman et al., 1992; Foster et al., 1994). Phosphorylation by aPKC- $\lambda$  and/or aPKC- $\zeta$  may enhance the activity of p190<sup>Rho-GAP</sup>, resulting in an increased conversion of RhoGTP to RhoGDP and stress fiber dissolution. Tyrosine phosphorylation of p190 by c-Src has been shown to be correlated with EGF-induced stress fiber disassembly (Chang et al., 1995). Evidence for a PKC-catalyzed serine/threonine phosphorylation of p190, however, is still lacking. Alternatively, aPKC- $\lambda$  and/or aPKC- $\zeta$  may enhance the RhoGDP level by inhibiting Rho-GDI, or exchange factors (GEF) acting on Rho, like SmgGDS, Rap1, Dbl, Ect2, and Ost (Hiraoka et al., 1992; Miki et al., 1993; Horii et al., 1994). However, models in which the Ras-induced disassembly of actin stress fibers are described as resulting exclusively from a Ras-mediated conversion of RhoGTP to RhoGDP are inconsistent with the findings demonstrating an activation of Rho by Ras as essential for transformation and mitogenesis by oncogenic Ras (Prendergast et al., 1995; Qui et al., 1995a,b; Olson et al., 1998).

CA mutants of Rac1 and RhoA enhance the transforming activity of Ras including the oncogene-induced morphological alterations (Khosravi-Far et al., 1995). The biological meaning of the reorganization of the actin cytoskeleton by transforming Ras as well as the role of RhoA in Ras transformed cells are not quite clear. As outlined above, activation of RhoA is required for transformation by Ras and expression of a CA mutant of RhoA enhances the transforming activity of Ras (Khosravi-Far et al., 1995). The fact, however, that oncogenic Ras causes a disassembly of actin stress fibers whereas CA RhoA promotes stress fiber formation indicates that oncogenic Ras somehow deregulates the normal Rho-mediated effects on the cytoskeleton. In Ras-transformed cells, the activation of Rho has been shown to be required for a suppression of p21Waf1/Kip which is upregulated in cells expressing oncogenic Ras (Olson et al., 1998), thus indicating that Rho

exerts other functions besides regulation of the actin cytoskeleton. This notion is supported by findings indicating that RhoA can mediate several distinct effector pathways and that transformation by RhoA and the ability to remodel the cytoskeleton are, to some extent, independent, e.g., transformation was found to correlate with Rho-associated kinase binding rather than stress fiber formation (Sahai et al., 1998). Thus, the Ras-mediated disassembly of actin stress fibers is not necessarily in conflict with the postulated activation of RhoA in Ras-transformed cells. Furthermore, expression of the Rho family member Rnd3/RhoE has been shown to result in a phenotype which strikingly resembles the phenotypic alterations caused by oncogenic Ras, i.e., cell rounding, loss of stress fibers, and decreased cell adhesion (Nobes et al., 1998). Recent results suggest that RhoE may act to inhibit signaling downstream of RhoA, by altering some RhoA-regulated responses, such as stress fiber formation, whereas other RhoA-mediated effects remain unaffected (Guasch et al., 1998).

The biochemical function of aPKC- $\lambda$  and aPKC- $\zeta$  in the Ras/Rac/Rho pathway remains to be elucidated. Evidence for PKC as an important regulator of cytoskeletal functions has been presented by numerous studies (Keenan and Kelleher, 1998). Stress fibers are associated with focal adhesion complexes where cells interact with the extracellular matrix. The interaction with the extracellular matrix is mediated by integrin receptors which are integral components of focal adhesion plaques (Schwartz et al., 1995). Activation of integrin receptors initiates a signaling cascade which has been shown to depend on stress fibers (Hynes, 1992; Rosales et al., 1995; Wu et al., 1995) and to cooperate with growth factor-mediated events (Clark and Brugge, 1995; Schwartz et al., 1995). An implication of PKC in focal adhesion formation and integrin-mediated signaling has been described (Clark and Brugge, 1995; Schwartz et al., 1995). By permitting anchorage-indepen-

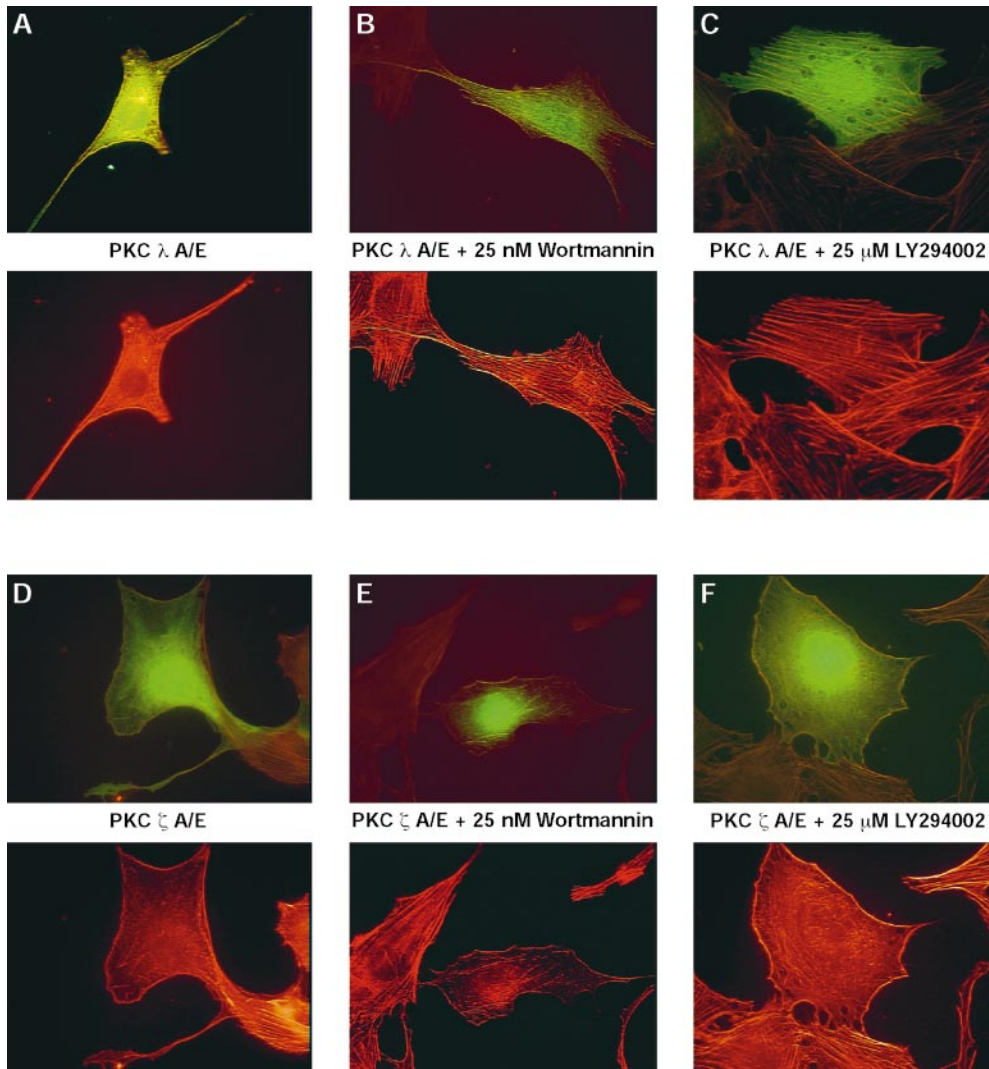


**Figure 9.** Evidence that atypical aPKC- $\lambda$  acts upstream of PI3K and Rac-1, whereas aPKC- $\zeta$  functions downstream of PI3K and Rac-1. Shown are representative fluorescence images of fibroblasts transiently expressing (CA) atypical aPKC- $\lambda$  (A–C). (A) (CA) aPKC- $\lambda$  alone, or (B) in the presence of 25 nM wortmannin, or (C) 25  $\mu$ M LY294002; (D) (CA) aPKC- $\zeta$  A119E alone, or (E) in the presence of 25 nM wortmannin, or (F) 25  $\mu$ M LY294002. 48 h post-transfection, cells were fixed and visualized as described in Materials and Methods. Representative cells of at least three different experiments are shown for all panels. Stacks of images were exported into Adobe Photoshop and printed as described above.

dent growth, transforming Ras may override the necessity for cell attachment. Evidence in support of this concept has been presented (Kang and Krauss, 1996). Both Src and Ras have been shown to act as important elements in inte-

grin-mediated signaling (Schlaepfer et al., 1998). Expression of oncogenic mutants of either protein may not only circumvent integrin receptor activation but may also lead to a disruption of focal adhesions and stress fibers as a result of a persistent activation of downstream elements of the integrin-regulated pathways, as had been suggested for v-Src (Fincham et al., 1995; Hildebrand et al., 1993).

We are grateful to A. Hall (London, UK), H. Mischak (Berlin, Germany), and J. Moscat (Madrid, Spain) for providing the plasmid pGST-N17Rac, pRc-CMV-PKC- $\lambda$  K275W, pCDNA3-PKC- $\zeta$  K275W-HA-tagged, and a full-length PKC- $\zeta$  cDNA, to S. Geley (Innsbruck, Austria) for subcloning pEFneoGFP-S65T, and to M. Karin (San Diego, CA) for plasmid pSR- $\alpha$ II L61 Ha-Ras. Furthermore, the authors wish to thank E. Preuss (Präsen-tation Dokumentation Lernsysteme, Innsbruck, Austria) for illustration.

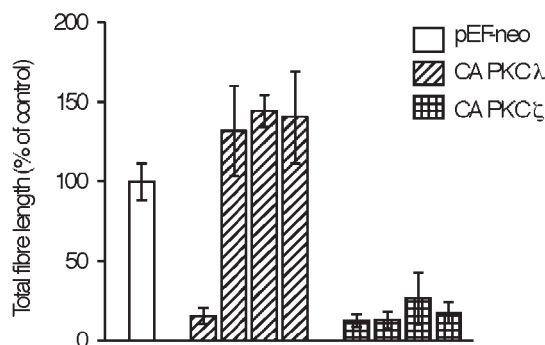


**Figure 10.** Quantitative evaluation of total fiber length. Effect of CA aPKC- $\lambda$  and aPKC- $\zeta$  alone, together with (DN) N17Rac, or

after treatment with the PI3K inhibitors wortmannin and LY294002. Total F-actin fiber length for all images were calculated as described in Fig. 4. Shown is a quantitative evaluation of total F-actin fiber length from fibroblasts expressing CA aPKC- $\lambda$  and aPKC- $\zeta$  mutants under the influence of (DN) N17 Rac-1, and the PI3K inhibitors wortmannin and LY294002. Final inhibitor concentrations are described above. Bars indicate means ( $\pm$  SEM) of at least three independent experiments with  $\sim$ 70–75 GFP-positive cells analyzed per coverslip.

This work was supported in part by grants from the Austrian Fond zur Förderung der wissenschaftlichen Forschung (FWF, P12547-MOB), des Sonderforschungsbereiches (SFB, F201, Biological communication systems, P12104-MED), and the Austrian Federal Bank (project 7399).

Received for publication 10 September 1998 and in revised form 24 December 1998.

## References

- Aktories, K., S. Braun, S. Roesener, I. Just, and A. Hall. 1989. The rho gene product expressed in *E. coli* is a substrate for botulinum ADP-ribosyltransferase C3. *Biochem. Biophys. Res. Commun.* 158:209–213.
- Arber, S., F.A. Barbayannis, H. Hanser, C. Schneider, C.A. Stanyon, O. Bernard, and P. Caroni. 1998. Regulation of actin dynamics through phosphorylation of cofilin by LIM-kinase. *Nature*. 393:805–809.
- Baier-Bitterlich, G., F. Überall, B. Bauer, F. Fresser, H. Wachter, H. Grunicke, G. Utermann, A. Altman, and G. Baier. 1996. PKC- $\theta$  isoenzyme selective stimulation of the transcription factor complex AP-1 in T-lymphocytes. *Mol. Cell. Biol.* 16:1842–1850.
- Bar-Sagi, D., and J.R. Feramisco. 1986. Induction of membrane ruffling and fluid-phase pinocytosis in quiescent fibroblasts by Ras proteins. *Science*. 233:1061–1068.
- Bjorkoy, G., M. Perander, A. Overvatn, and T. Johansen. 1997. Reversion of Ras- and phosphatidylcholine-hydrolyzing phospholipase C-mediated transformation of NIH 3T3 cells by a dominant interfering mutant of protein kinase C lambda is accompanied by the loss of constitutive nuclear mitogen-activated protein kinase/extracellular signal-regulated kinase activity. *J. Biol. Chem.* 272:11557–11565.
- Boguski, M.S., R.C. Hardison, S. Schwartz, and W. Miller. 1992. Analysis of conserved domains and sequences motifs in cellular regulatory proteins and locus control regions using new software tools for multiple alignment and visualization. *New Biol.* 4:247–260.
- Burridge, K., K. Fath, T. Kelly, G. Nuckolls, and C. Turner. 1988. Focal adhesions: transmembrane junctions between the extracellular matrix and the cytoskeleton. *Annu. Rev. Cell Biol.* 4:487–525.
- Burridge, K., C.E. Turner, and L.H. Romer. 1992. Tyrosine phosphorylation of paxillin and pp125FAK accompanies cell adhesion to extracellular matrix: role in cytoskeletal assembly. *J. Cell Biol.* 119:893–903.
- Chang, J.H., S. Gill, J. Settleman, and S.J. Parsons. 1995. c-Src regulates the simultaneous rearrangement of actin cytoskeleton, p190RhoGAP, and p120RasGAP following epidermal growth factor stimulation. *J. Cell Biol.* 130:355–368.
- Chant, J., and L. Stowers. 1995. GTPase cascades choreographing cell behavior: movement, morphogenesis, and more. *Cell*. 81:1–4.
- Chardin, P., P. Boquet, P. Maduale, M.R. Popoff, E.J. Rubin, and D.M. Gill. 1989. The mammalian G protein rhoC is ADP-ribosylated by *Clostridium botulinum* exoenzyme C3 and affects actin microfilaments in Vero cells. *EMBO (Eur. Mol. Biol. Organ.) J.* 8:1087–1092.
- Chun, J.S., and B.S. Jacobson. 1992. Requirement for diacylglycerol and protein kinase C in HELA cell-substratum adhesion and their feedback amplification of arachidonic acid production for optimum cell spreading. *Mol. Biol. Cell.* 4:271–281.
- Clark, E.A., and J.S. Brugge. 1995. Integrins and signal transduction pathways: the road taken. *Science*. 268:233–239.
- Cubitt, A.B., R. Heim, S.R. Adams, A.E. Boyd, L.A. Gross, and R.Y. Tsien. 1995. Understanding, improving and using green fluorescent proteins. *Trends Biochem. Sci.* 20:448–455.
- Dartsch, P.C., M. Ritter, D. Haussinger, and F. Lang. 1994. Cytoskeletal reorganization in NIH3T3 fibroblasts expressing the Ras oncogene. *Eur. J. Cell Biol.* 63:316–325.
- Diaz-Meco, M.T., M.M. Municio, E. Berra, S. Frutos, L. Sanzo, and J. Moscat. 1994. Evidence for the in vitro and in vivo interaction of Ras with protein kinase zeta. *J. Biol. Chem.* 269:31706–31710.
- Feig, L., and B. Schaffhausen. 1994. The hunt for Ras targets. *Nature*. 370:508–509.
- Felice, G.R., P. Eason, M.V. Nermut, and S. Kellie. 1990. pp60src association with the cytoskeleton induces actin reorganization without affecting polymerization status. *Eur. J. Cell Biol.* 52:47–59.
- Fincham, V.J., J.A. Wyke, and M.C. Frame. 1995. v-Src-induced degradation of focal adhesion kinase during morphological transformation of chicken embryo fibroblasts. *Oncogene*. 10:2247–2252.
- Foster, R., K.Q. Hu, D.A. Shaywitz, and J. Settleman. 1994. p190 rhoGAP, the major rasGAP-associated protein, binds GTP directly. *Mol. Cell. Biol.* 14:7173–7181.
- Gomez, J., L. Rodriguez-Borlado, C. Martinez, A. Silva, M. Fresno, A.C. Carrera, C. Eicher-Streiber, and A. Rebello. 1997. IL-2 signaling controls actin reorganization through Rho-like protein family, phosphatidylinositol 3-kinase, and protein kinase C-zeta. *J. Immunol.* 158:1516–1522.
- Guan, J.T., J.E. Trevithick, and R.O. Hynes. 1991. Fibronectin/integrin interaction induces tyrosine phosphorylation of a 120-kDa protein. *Cell Regul.* 2:951–964.
- Guasch, R.M., P. Scambler, G.E. Jones, and A.J. Ridley. 1998. RhoE regulates actin cytoskeleton organization and cell migration. *Mol. Cell. Biol.* 18:4761–4771.
- Hall, A. 1990. The cellular function of small GTP-binding proteins. *Science*. 249:635–640.
- Hildebrand, J.D., M.D. Schaller, and J.T. Parsons. 1993. Identification of sequences required for the efficient localization of the focal adhesion kinase, pp125FAK, to cellular focal adhesions. *J. Cell Biol.* 23:993–1005.
- Hiraoka, K., K. Kaibuchi, S. Ando, T. Musha, K. Takaishio, T. Mizuno, L. Menard, E. Tomhave, and J. Didsbury. 1992. Both stimulatory and inhibitory GDT/GTP exchange proteins, smg GDS and rho GDI, are active on multiple small GTP-binding proteins. *Biochem. Biophys. Res. Commun.* 182:921–930.
- Horii, Y., J.F. Beeler, K. Sakaguchi, M. Tachibana, and T. Miki. 1994. A novel oncogene, ost, encodes a guanine nucleotide exchange factor that potentially links rho and rac signaling pathways. *EMBO (Eur. Mol. Biol. Organ.) J.* 13:4776–4786.
- Hynes, R.O. 1992. Integrins: versatility, modulation, and signaling in cell adhesion. *Cell*. 69:11–25.
- Joneson, T., and D. Bar-Sagi. 1997. Ras effectors and their role in mitogenesis and oncogenesis. *J. Mol. Med.* 75:587–593.
- Kamper, S., K. Hellbert, A. Villunger, W. Doppler, G. Baier, H.H. Grunicke, and F. Überall. 1998. Transcriptional activation of c-fos by oncogenic Ha-Ras in mouse mammary epithelial cells requires the combined activities of PKC- $\lambda$ ,  $\epsilon$ , and  $\zeta$ . *EMBO (Eur. Mol. Biol. Organ.) J.* 17:4046–4055.
- Kang, J.S., and R.S. Krauss. 1996. Ras induces anchorage-independent growth by subverting multiple adhesion regulated cell cycle events. *Mol. Cell. Biol.* 16:3370–3380.
- Keenan, C., and D. Kelleher. 1998. Protein kinase C and the cytoskeleton. *Cell Signal.* 10:225–232.
- Khosravi-Far, R., P.A. Solski, G.J. Clark, M.S. Kinch, and C.J. Der. 1995. Activation of rac1, rhoA, and mitogen-activated protein kinases is required for ras transformation. *Mol. Cell. Biol.* 15:6443–6453.
- Kornberg, L., H.S. Earp, J.T. Parsons, M. Schaller, and R.L. Juliano. 1992. Cell adhesion or integrin clustering increases phosphorylation of a focal adhesion-associated tyrosine kinase. *J. Biol. Chem.* 267:23439–23442.
- Kumar, C.C., C. Rogers-Prorock, J. Kelly, Z. Dong, J.-J. Lin, L. Armstrong, H.-F. Kung, M.J. Weber, and A. Afonso. 1995. SCH51344 inhibits Ras transformation by a novel mechanism. *Cancer Res.* 55:5106–5117.
- Martiny-Baron, G., M.G. Kazanietz, H. Mischak, P.M. Blumberg, G. Kochs, H. Hug, D. Marme, and C. Schaechtele. 1993. Selective inhibition of protein kinase C isoenzymes by the indolocarbazole Goe 6976. *J. Biol. Chem.* 268:9194–9197.
- Mellström, K., C.H. Heldin, and B. Westermark. 1988. Induction of circular membrane ruffling on human fibroblasts by platelet-derived growth factor. *Exp. Cell Res.* 177:347–359.
- Miki, T., C.L. Smith, J.E. Long, A. Eva, and T.P. Fleming. 1993. Oncogene ect-2 is related to regulators of small GTP-binding proteins. *Nature*. 362:462–465.
- Mogi, A., M. Hatai, H. Soga, S. Takenoshita, Y. Nagamachi, J. Fujimoto, T. Yamamoto, J. Yokota, and Y. Yaoi. 1995. Possible role of protein kinase C in the regulation of intracellular stability of focal adhesion kinase in mouse 3T3 cells. *FEBS (Fed. Eur. Biochem. Soc.) Lett.* 373:135–140.
- Morris, J.D.H., B. Price, A.C. Lloyd, A.J. Self, C.H. Marshall, and A. Hall. 1989. Scrape-loading of Swiss 3T3 cells with Ras protein rapidly activates protein kinase C in the absence of phosphoinositide hydrolysis. *Oncogene*. 4:27–31.
- Nobes, C.D., and A. Hall. 1994. Regulation and function of the rho subfamily of small GTPases. *Curr. Opin. Genet. Dev.* 4:71–81.
- Nobes, C.D., and A. Hall. 1995. Rho, rac, and cdc42 GTPase regulates the assembly of multimolecular focal complexes associated with actin stress fibres, lamellipodia, and filopodia. *Cell*. 81:53–62.
- Nobes, C.D., I. Lauritzen, M.G. Mattei, A. Hall, and P. Chardin. 1998. A new member of the Rho family, Rnd1, promotes disassembly of actin filament structures and loss of cell adhesion. *J. Cell Biol.* 141:187–197.
- Olson, M.F., H.F. Paterson, and C.J. Marshall. 1998. Signals from Ras and Rho GTPases interact to regulate expression of p21Waf1/Cip1. *Nature*. 394:295–299.
- Paterson, H.F., A.J. Self, M.D. Garrett, I. Just, K. Aktories, and A. Hall. 1990. Microinjection of recombinant p21rho induces rapid changes in cell morphology. *J. Cell Biol.* 111:1001–1007.
- Prendergast, G.C., and J.B. Gibbs. 1993. Pathways of Ras function: connections to the actin cytoskeleton. *Adv. Cancer Res.* 62:19–64.
- Prendergast, G.C., R. Khosravi-Far, P.A. Solski, H. Kurzawa, P.F. Lebowitz, and C.J. Der. 1995. Critical role of Rho in cell transformation by oncogenic Ras. *Oncogene*. 10:2289–2296.
- Qui, R.G., J. Chen, D. Kim, F. McCormick, and M. Symons. 1995a. An essential role for rac in Ras transformation. *Nature*. 374:457–459.
- Qui, R.G., J. Chen, D. Kim, F. McCormick, and M. Symons. 1995b. A role of rho in Ras transformation. *Proc. Natl. Acad. Sci. USA*. 92:11781–11785.
- Rankin, S., and E. Rozengurt. 1994. Platelet-derived growth factor modulation of focal adhesion kinase p125FAK and paxillin tyrosine phosphorylation in Swiss 3T3 cells. Bell-shaped dose response and cross-talk with bombesin. *J. Biol. Chem.* 269:704–710.
- Ridley, A.J. 1995. Rho-related proteins: actin cytoskeleton and cell cycle. *Curr. Opin. Genet. Dev.* 5:24–30.
- Ridley, A.J., H.F. Paterson, C.L. Johnston, D. Diekmann, and A. Hall. 1992. The small GTP-binding protein rac regulates growth factor-induced membrane ruffling. *Cell*. 70:401–410.
- Ridley, A.J., and A. Hall. 1992. The small GTP-binding protein rho regulates

- the assembly of focal adhesions and actin stress fibres in response to growth factors. *Cell*. 70:389–399.
- Rodriguez-Viciana, P., P.H. Warne, R. Dhand, B. Vanhaesebroeck, I. Gout, M.J. Fry, M.D. Waterfield, and J. Downward. 1994. Phosphatidylinositol-3-OH kinase as a direct target of Ras. *Nature*. 370:527–532.
- Rosales, C., V. O'Brien, L. Kornberg, and R. Juliano. 1995. Signal transduction by cell adhesion receptors. *Biochim. Biophys. Acta*. 1242:77–98.
- Rosen, A., K.F. Keenan, M. Thelen, A.C. Nairn, and A. Aderem. 1990. Activation of protein kinase C results in the displacement of its myristoylated, alanine-rich substrate from punctate structures in macrophage filopodia. *J. Exp. Med.* 92:1211–1215.
- Rubin, E.J., D.M. Gill, P. Boquet, and M.R. Popoff. 1988. Functional modification of a 21 kDa G protein when ADP-ribosylated by exoenzyme C3 of *Clostridium botulinum*. *Mol. Cell. Biol.* 8:418–426.
- Sahai, E., A.S. Alberts, and R. Treisman. 1998. RhoA effector mutants reveal distinct effector pathways for cytoskeletal reorganization, SRF activation and transformation. *EMBO (Eur. Mol. Biol. Organ.) J.* 17:1350–1361.
- Schlaepfer, D.D., K.C. Jones, and T. Hunter. 1998. Multiple Grb2-mediated integrin-stimulated signaling pathways to ERK2/mitogen-activated protein kinase: summation of both c-Src- and focal adhesion kinase-initiated tyrosine phosphorylation events. *Mol. Cell. Biol.* 18:2571–2585.
- Schwartz, M.A., M.D. Schaller, and M.H. Ginsberg. 1995. Integrins: emerging paradigms of signal transduction. *Annu. Rev. Cell. Dev. Biol.* 11:549–599.
- Settleman, J., C.F. Albright, L.C. Foster, and R.A. Weinberg. 1992. Association between GTPase activators for Rho and Ras families. *Nature*. 359:153–154.
- Shinjo, K., J.G. Koland, M.J. Hart, V. Narasimhan, D.I. Johnson, T. Evans, and R.A. Cerione. 1990. Molecular cloning of the gene for the human placental GTP-binding protein Gp (G25K): identification of this GTP-binding protein as the human homolog of the yeast cell-division-cycle protein CDC42. *Proc. Natl. Acad. Sci. USA*. 87:9853–9857.
- Smith-Sinnett, J., I. Zachary, A.M. Valverde, and E. Rozengurt. 1993. Bombesin stimulation of p125 focal adhesion kinase tyrosine phosphorylation. *J. Biol. Chem.* 268:14261–14268.
- Toullec, D., P. Pianetti, H. Coste, P. Bellevergue, T. Grand-Perret, M. Ajakane, V. Baudet, P. Boissin, E. Brousier, F. Loriolle, L. Duhamel, D. Charon, and J. Kirilovsky. 1991. The bisindolylmaleimide GFX 109203 X is a potent and selective inhibitor of protein kinase C. *J. Biol. Chem.* 266:15771–15781.
- Überall, F., S. Giselbrecht, K. Hellbert, F. Fresser, B. Bauer, M. Gschwendt, H.H. Grunicke, and G. Baier. 1997. Conventional PKC- $\alpha$ , novel PKC- $\epsilon$  and PKC- $\theta$ , but not atypical PKC- $\lambda$  are MARCKS kinases in intact NIH3T3 fibroblasts. *J. Biol. Chem.* 272:4072–4078.
- Vuori, K., and E. Ruoslati. 1993. Activation of protein kinase C precedes  $\alpha 5 \beta 1$  integrin-mediated cell spreading on fibronectin. *J. Biol. Chem.* 268:21459–21462.
- Wu, C., V.M. Keivens, T.E. O'Toole, J.A. McDonald, and M.H. Ginsberg. 1995. Integrin activation and cytoskeletal interaction are essential for the assembly of fibronectin matrix. *Cell*. 83:715–724.
- Yang, N., O. Higuchi, K. Ohashi, K. Nagata, A. Wada, K. Kangawa, E. Nishida, and K. Mizuno. 1998. Cofilin phosphorylation by LIM-kinase 1 and its role in Rac-mediated actin reorganization. *Nature*. 393:809–812.
- Zachary, I., and E. Rozengurt. 1992. Focal adhesion kinase (p125FAK): a point of convergence in the action of neuropeptides, integrins and oncogenes. *Cell*. 71:891–894.

